



## Open Archive Toulouse Archive Ouverte

OATAO is an open access repository that collects the work of Toulouse researchers and makes it freely available over the web where possible

This is an author's version published in:

<http://oatao.univ-toulouse.fr/24718>

### Official URL

DOI : <https://doi.org/10.1109/ULTSYM.2018.8580075>

**To cite this version:** Kim, Jong-Hoon and Mamou, Jonathan and Kouamé, Denis and Achim, Alin and Basarab, Adrian *Reconstruction of Quantitative Acoustic Microscopy Images from RF Signals Sampled at Innovation Rate*. (2018) In: IEEE International Ultrasonics Symposium (IUS 2018), 22 October 2018 - 25 October 2018 (Kobe, Japan).

Any correspondence concerning this service should be sent to the repository administrator: [tech-oatao@listes-diff.inp-toulouse.fr](mailto:tech-oatao@listes-diff.inp-toulouse.fr)

# Reconstruction of Quantitative Acoustic Microscopy Images from RF Signals Sampled at Innovation Rate

J.-H. Kim<sup>1</sup>, J. Mamou<sup>2</sup>, D. Kouamé<sup>1</sup>, A. Achim<sup>3</sup>, and A. Basarab<sup>1</sup>

<sup>1</sup>IRIT UMR CNRS 5505, University of Toulouse, CNRS, INPT, UPS, UT1C, UT2J, France

<sup>2</sup>Frederic L. Lizzi Center for Biomedical Engineering, Riverside Research, New York, NY 10038, USA

<sup>3</sup>Visual Information Lab, Merchant Venturers School of Engineering, University of Bristol, BS8 1UB, Bristol, UK

**Abstract**—The principle of quantitative acoustic microscopy (QAM) is to form two-dimensional acoustic parameter maps from a collection of radiofrequency (RF) signals acquired by raster scanning a biological sample. Despite their relatively simple structure, i.e. two main reflections, QAM RF signals are currently sampled at very high frequencies, e.g., at 2.5 GHz for QAM system employing a single-element transducer with a center frequency of 250-MHz. The use of such high sampling frequencies is challenging because of the potentially large amount of acquired data and the cost of the necessary analog to digital converters. In this work, we propose a sampling scheme based on the finite rate of innovation theory that exploits the limited numbers of degrees of freedom of QAM RF signals and allows the reconstruction of accurate acoustic maps from a very limited number of samples.

**Index Terms**—Scanning Acoustic Microscopy, finite rate of innovation, auto-regressive model

## I. INTRODUCTION

Quantitative Acoustic Microscopy (QAM) uses high frequency ultrasound waves to investigate the mechanical properties of biological tissues at microscopic scale [1]–[4]. Currently, the acquisition process in QAM requires a raster scan of the sample, resulting into a large amount of RF data acquired by transmitting short ultrasound pulses into a thin section of soft tissue affixed to a microscopy slide. At each spatial position, the received RF echo consists of two main reflections due to the water-tissue and tissue-glass interfaces. These reflections are time shifted, frequency attenuated linearly, and scaled versions of a reference reflection signal obtained from a water-glass interface. Two-dimensional (2D) acoustic maps are thus estimated from an RF data cube using for example an autoregressive (AR) model for each RF signal [5].

Despite their limited degrees of freedom, QAM RF signals are currently sampled beyond the Nyquist rate (i.e. approximately 800 MHz) at 2.5 GHz for 250-MHz scanners extending from 100 to 400 MHz. This results in a number of practical issues, such as a large amount of acquired data or the cost and the complexity of the A/D converters. In our previous study in [6], we demonstrated that adapting the compressive sensing framework to QAM in the spatial domain allows to drastically decrease the amount of acquired data. In this work, we propose a sampling scheme in the temporal domain able to reduce drastically the number of samples per RF signal required to

reconstruct accurate acoustic maps in QAM. The proposed approach is based on the finite rate of innovation (FRI) theory [7], that provides theoretical guarantees for reconstructing FRI signals, i.e. described by a limited number of parameters, from a small number of samples acquired at the innovation rate. Interestingly, it has been shown that such a reconstruction is even possible in the case of non-bandlimited signals such as stream of Diracs [7].

The proposed sampling and reconstruction methods for QAM RF signals is evaluated on experimental data obtained from an excised lymph node of a breast cancer patient. The resulting 2D speed of sound maps are compared to those classically computed from the fully sample RF data cubes. We thus show that the sampling frequency currently used in SAM can be reduced by a factor of 15 (i.e., 20.3% of Nyquist rate) without degrading the quality of the 2D acoustic maps.

The remainder of this paper is structured as follows. Section II gives a brief background on sampling and reconstruction of FRI signals. Section III introduces the FRI model proposed for QAM, as well as the AR estimator used to compute acoustic parameters. Simulation results are reported in Section IV, before concluding the paper in Section V.

## II. BASICS OF FRI SIGNAL SAMPLING AND RECONSTRUCTION

Signals with a limited number of degrees of freedom occur in various applications such as astronomy, radar or ultrasound imaging [8]–[12]. Commonly called signals with FRI, they have the following  $\tau$ -periodic parametric form:

$$x(t) = \sum_{k \in \mathbb{Z}} \sum_{l=1}^L a_l h(t - t_l - k\tau), \quad (1)$$

where  $h(t)$  is a possibly non-bandlimited pulse considered known and repeated at times  $t_l$  and scaled by the amplitudes  $a_l$ . Starting from the seminal paper of Vetterli *et al.* [7], a rich literature exists on the reconstruction of these type of signals from a limited number of samples. In contrast to the classical sampling theory based on the well-known Shannon-Nyquist theorem that relates the number of samples required to the signal bandwidth, the number of measurements required

for FRI signals is dictated by the rate of innovation, i.e. the number of parameters defining  $x(t)$  over one period. Interestingly, it has thus been shown that even non-bandlimited signals such as streams of Diracs can be accurately reconstructed from a limited number of samples [7]. The sampling and reconstruction process typically consists in (i) properly choosing a sampling kernel (e.g., sum of sinc functions in the frequency domain [12]), (ii) uniform sampling, (iii) computing Fourier series coefficients from the acquired samples and (iv) estimating the unknown time delays and amplitudes that allows the perfect reconstruction of the FRI signal. The latter is commonly achieved using the annihilating filter [13], [14], able to estimate the signal's degrees of freedom from the critical number of sample, i.e.  $2L$  for the model in (1).

### III. QAM RECONSTRUCTION FROM SAMPLES AT INNOVATION RATE

#### A. Signal model

In QAM, RF signals consists of two main reflections due the water-tissue and tissue-glass interfaces. They can be thus modeled by the sum of two time-delayed, frequency-dependent attenuated version of a reference RF pulse [5]. The non-attenuated reference pulse, denoted by  $h$  hereafter and assumed to be known, is commonly measured on the same time as the sample scanning, from a region without sample, i.e. presenting only one water-glass interface. As in most of the existing works, the attenuation is considered herein to vary linearly with the frequency. Written in a  $\tau$ -periodic version, the QAM RF signal model is as follows:

$$\begin{aligned} x(t) &= \sum_{m \in \mathbb{Z}} \sum_{l=1}^2 a_l h^{(l)}(t - t_l - m\tau) \\ &= \sum_{k \in \mathbb{Z}} \left\{ \frac{1}{\tau} H \left[ \frac{2\pi k}{\tau} \right] \sum_{l=1}^2 a_l e^{\frac{-j2\pi k t_l - 2\pi k \beta_l}{\tau}} \right\} e^{\frac{j2\pi k t}{\tau}} \quad (2) \\ &\triangleq \sum_{k \in \mathbb{Z}} X[k] e^{\frac{j2\pi k t}{\tau}}, \end{aligned}$$

where  $h^{(l)}$  are frequency-dependent attenuated versions of the reference pulse  $h$ ,  $\beta_l$  are the frequency attenuation coefficients,  $a_l$  are the amplitudes,  $t_l$  the time delays,  $H$  is the continuous time Fourier transform of  $h$  and  $k$  is the frequency variable. Without loss of generality, we assume herein  $\beta_1$  equal to 0. Thus, the unknown parameters are  $a_1$ ,  $a_2$ ,  $t_1$ ,  $t_2$  and  $\beta_2$ . Note that compared to the model in (1), the QAM model has an additional degree of freedom related to the frequency-dependent attenuation. In (2), the last line represents the Fourier series expansion of  $x(t)$ , with  $X[k]$  the Fourier series coefficients. By identification, one can easily relate  $X[k]$  to the unknown parameters, i.e.  $X[k] = \frac{1}{\tau} H[2\pi k/\tau] \sum_{l=1}^2 a_l e^{\frac{-j2\pi k t_l - 2\pi k \beta_l}{\tau}}$ .

#### B. Sampling procedure

The sampling procedure used in this work is similar to the one proposed in [12]. The main idea is to sample uniformly the demodulated QAM signal using a finite support Sum of Sincs (SoS) sampling kernel and to relate these sample through

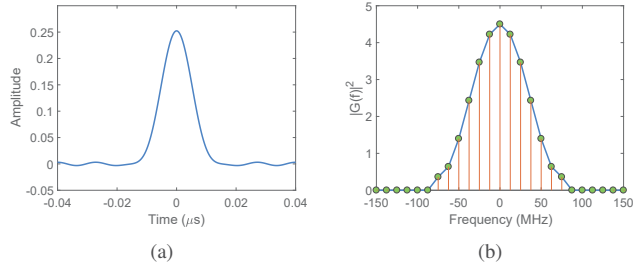


Fig. 1. Example of SoS sampling kernel in temporal and frequency domain.

a linear model to the Fourier series coefficients  $X[k]$ . In the Fourier domain, the SoS sampling kernel (denoted by  $g(t)$  in the time domain) is given by

$$G(\omega) = \frac{\tau}{\sqrt{2\pi}} \sum_{k \in \mathbb{Z}} b_k \text{sinc} \left( \frac{\omega}{2\pi} - k \right), \quad (3)$$

where  $b_k$  is a smoothing window (Hamming window was used in our experiments). An example of SoS sampling kernel is shown in Fig. 1, in both the temporal and frequency domains. We denote by  $c[n]$  the sampled version of  $x(t)$  with the sampling kernel  $g(t)$  and a sampling period  $T$ :

$$\begin{aligned} c[n] &= \int_{-\infty}^{\infty} x(t) g^*(t - nT) dt = \langle g(t - nT), x(t) \rangle \\ &= \sum_{k \in \mathbb{Z}} X[k] e^{\frac{j2\pi k n T}{\tau}} G^* \left[ \frac{2\pi k}{\tau} \right] \quad (4) \end{aligned}$$

One may observe that if the sampling frequency and the sampling kernel are chosen properly so that  $G^* \left[ \frac{2\pi k}{\tau} \right]$  is different from zero only for a finite number of  $\frac{2\pi k}{\tau}$  values, than the sum in (4) becomes finite. Thus, the Fourier series coefficients  $X[k]$  can be computed from the digital samples  $c[n]$  by applying the inverse of a correction matrix to the discrete Fourier transform of  $c[n]$  (see [12] for more details).

#### C. Reconstruction method

The computation of the acoustic parameters is based on the estimation of the amplitudes, delays and frequency attenuation coefficients given in the QAM model (2). The estimation of the latter is obtained from the Fourier series coefficients  $X[k]$  through an AR model as suggested in [5]. Defining by  $N_k$  the ratio between  $X[k]$  and  $H[2\pi k/\tau]$ , we obtain:

$$N_k = \sum_{l=1}^2 a_l e^{\{2\pi \Delta f [-\beta_l - j t_l]\} k} = \sum_{l=1}^2 a_l \lambda_l^k, \quad (5)$$

where  $\Delta f$  is the frequency spacing and  $\lambda_l$  stands for  $\exp\{2\pi \Delta f [-\beta_l - j t_l]\}$ . Denoting by  $\epsilon_k$  the error term and by  $s_f$  the AR coefficients, the AR model for QAM proposed in [5] is:

$$N_k = \sum_{l=1}^2 s_l N_{k-l} + \epsilon_k \quad (6)$$

The coefficient of the AR model are found using our inverse model and the acoustic parameters are directly estimates from the AR parameters as in [5]. For instance, the speed of sound,  $c$ , is estimated using:

$$c = c_w \frac{\text{imag}(\log(\lambda_{i_1}))}{\text{imag}(\log(\lambda_{i_1})) + \text{imag}(\log(\lambda_{i_2}))}, \quad (7)$$

where  $c_w$  is the speed of sound in the coupling medium (i.e., water). Eq. (7) is derived from first principles by converting the phase differences between the reference pulse and each reflection in the time domain [5].

#### IV. RESULTS

In this section, the sampling process is firstly illustrated, followed by its qualitative and quantitative validation in achieving reliable 2D acoustic parameter maps.

##### A. Example of QAM RF signal sampling at innovation rate

In this section we illustrate the sampling procedure of a QAM RF signal at the innovation rate. The reference signal in Fig. 2(a) was obtained by averaging 25 neighboring RF signal selected from a region void of sample. It thus consists in only one reflection from the water-glass interface. In contrast to this reference RF signal, the RF QAM signals reflected by the tissue sample consist of two reflections, as shown in Fig. 2(a). In addition, the time delays between the reference signal and two reflections of the QAM signal result from the variation of the speed of sound during the flight within the different media. The sampling procedure, which consists of demodulation, SoS filtering and uniform sampling, was designed to give access to Fourier coefficients in the  $6dB$  bandwidth highlighted in Fig. 2(b). The resulting samples denoted by  $c[n]$  in the previous section, 13 of them in this example, are shown in Fig. 2(c-d) for the real and complex part of the sampled signal.

##### B. Acoustic parameter maps

In this section, we evaluate the quality of the 2D acoustic maps reconstructed from QAM RF signals sampled following the proposed scheme against the ones estimated from fully sampled RF data cubes. Note that only the speed of sound is considered in this paper, but the results are similar for other parameters such as the acoustic impedance or the acoustic attenuation. The experiment was based on data acquired from an *ex vivo* lymph node sample obtained from a breast-cancer patient, with a QAM system operating at 250 MHz center frequency. The fully sampled volume was obtained by sampling each RF signal at 2.5 GHz, yielding 200 samples at each scan location. The spatial raster scanning step was 2 by  $2\mu\text{m}$ , resulting into a data cube of size  $1000 \times 600 \times 200$  samples. The same data was sampled using the proposed method with the same spatial step size but with temporal sampling frequencies of 162.5 MHz, 137.5 MHz and 112.5 MHz, corresponding to respectively 13, 11 and 9 samples per QAM RF signal. These correspond to 20.3%, 17.2% and 14.1% of Nyquist rate (800 MHz) of the RF signal respectively. Fig. 3 illustrates the 2D speed of sound maps obtained from the four data cubes.

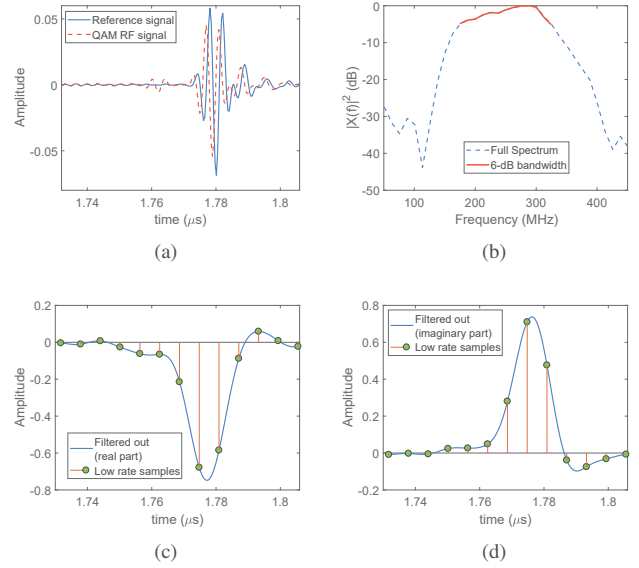


Fig. 2. (a) Example of QAM RF signals in the time domain, (b) Fourier transform of the reference signal in (a) highlighting the  $6dB$  bandwidth, (c) real and (d) imaginary parts of the demodulated sampled signal using SoS sampling kernel.

Number of samples	13	11	9
Sampling frequency (MHz)	162.5	137.5	112.5
Fraction of Nyquist rate in %	20.3	17.2	14.1
NRMSE	0.142	0.183	0.195
PSNR (dB)	32.05	29.82	29.28

TABLE I  
QUANTITATIVE RESULTS COMPUTED BETWEEN THE SoS MAP FROM FULLY SAMPLED RF DATA CUBE AND THOSE OBTAINED FROM QAM RF SIGNAL SAMPLED AT LOW RATES: 162.5 MHz (13 SAMPLES PER RF SIGNAL), 137.5 MHz (11 SAMPLES PER RF SIGNAL) AND 112.5 MHz (9 SAMPLES PER RF SIGNAL).

In spite of the much lower sampling rate, no salient visual difference exists between the 2D maps, except for a moderate degradation visible in the 2D maps reconstructed from only 9 samples per RF signal. These observations are quantitatively confirmed by standard quality metrics (i.e., normalized root mean square error and peak signal to noise ratio) shown in Table I.

#### V. CONCLUSIONS

The objective of this work was to combine a low rate RF signal sampling procedure with an AR model-based parametric acoustic map reconstruction in QAM imaging. Both approaches were based on a parametric modelisation of the QAM RF signals with a limited number of degrees of freedom, the amplitudes, delays and frequency-dependent attenuation coefficients. We show encouraging results proving that 2D acoustic maps can be reconstructed despite sampling frequencies more than 15 times lower than the one classically used within existing imaging systems and more than 5 times lower than required by the Nyquist criterion. Thus, the proposed framework could significantly reduce costs and experimental

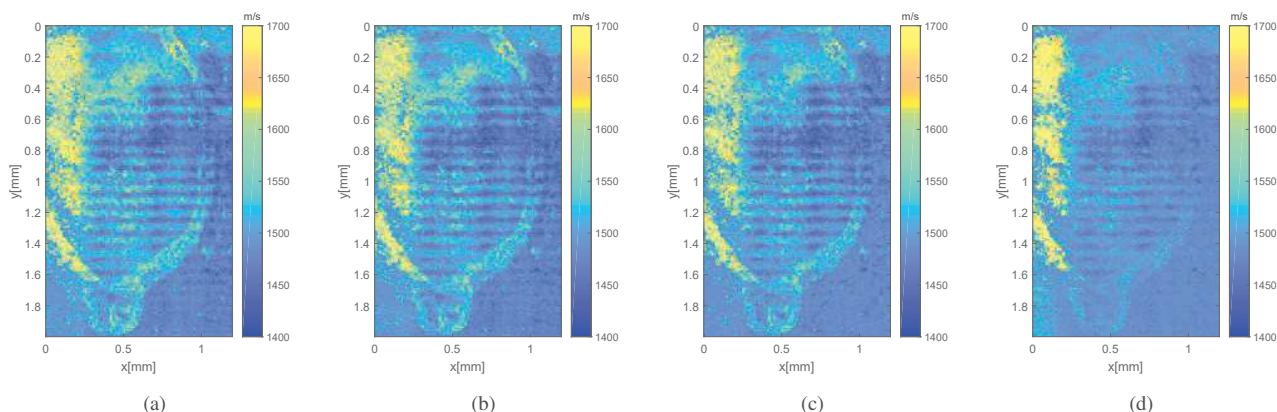


Fig. 3. Two-dimensional speed of sound maps obtained from complete data (a), our FRI approach with sampling frequency of 162.5 MHz (b), 137.5 MHz (c), and 112.5 MHz (d). Quantitative accuracy measurements computed from these speed of sound maps are given in Tab. I.

challenges in current QAM systems because of the current need for ultra-precise and fast sampling cards.

#### REFERENCES

- [1] S. Irie, K. Inoue, K. Yoshida, J. Mamou, K. Kobayashi, H. Maruyama, and T. Yamaguchi, "Speed of sound in diseased liver observed by scanning acoustic microscopy with 80mhz and 250mhz," *The Journal of the Acoustical Society of America*, vol. 139, p. 512–519, January 2016.
- [2] J. Mamou, D. Rohrbach, E. Saegusa-Becroft, E. Yanagihara, J. Machi, and E. J. Feleppa, "Ultrasound-scattering models based on quantitative acoustic microscopy of fresh samples and unstained fixed sections from cancerous human lymph nodes," in *2015 IEEE International Ultrasonics Symposium (IUS)*, pp. 1–4, Oct 2015.
- [3] D. Rohrbach, H. O. Lloyd, R. H. Silverman, R. Urs, and J. Mamou, "Acoustic-property maps of the cornea for improved high-frequency ultrasound corneal biometric accuracy," in *2015 IEEE International Ultrasonics Symposium (IUS)*, pp. 1–4, Oct 2015.
- [4] D. Rohrbach, A. Jakob, H. O. Lloyd, S. H. Tretbar, R. H. Silverman, and J. Mamou, "A novel quantitative 500-mhz acoustic microscopy system for ophthalmologic tissues," *IEEE Transactions on Biomedical Engineering*, vol. 64, pp. 715–724, March 2017.
- [5] D. Rohrbach and J. Mamou, "Autoregressive signal processing applied to high-frequency acoustic microscopy of soft tissues," *IEEE Transactions on Ultrasonics, Ferroelectrics, and Frequency Control*, 2018, in press.
- [6] J. Kim, J. Mamou, P. R. Hill, N. Canagarajah, D. Kouamé, A. Basarab, and A. Achim, "Approximate message passing reconstruction of quantitative acoustic microscopy images," *IEEE Transactions on Ultrasonics, Ferroelectrics, and Frequency Control*, vol. 65, pp. 327–338, March 2018.
- [7] M. Vetterli, P. Marziliano, and T. Blu, "Sampling signals with finite rate of innovation," *IEEE Transactions on Signal Processing*, vol. 50, pp. 1417–1428, Jun 2002.
- [8] J. Oñativia, S. R. Schultz, and P. L. Dragotti, "A finite rate of innovation algorithm for fast and accurate spike detection from two-photon calcium imaging," *Journal of Neural Engineering*, vol. 10, no. 4, p. 046017, 2013.
- [9] S. Rudresh and C. S. Seelamantula, "Finite-rate-of-innovation-sampling-based super-resolution radar imaging," *IEEE Transactions on Signal Processing*, vol. 65, pp. 5021–5033, Oct 2017.
- [10] X. Wei and P. L. Dragotti, "Fresh x2014;fri-based single-image super-resolution algorithm," *IEEE Transactions on Image Processing*, vol. 25, pp. 3723–3735, Aug 2016.
- [11] H. Pan, T. Blu, and M. Vetterli, "Towards generalized fri sampling with an application to source resolution in radioastronomy," *IEEE Transactions on Signal Processing*, vol. 65, pp. 821–835, Feb 2017.
- [12] R. Tur, Y. C. Eldar, and Z. Friedman, "Innovation rate sampling of pulse streams with application to ultrasound imaging," *IEEE Transactions on Signal Processing*, vol. 59, pp. 1827–1842, April 2011.
- [13] P. Stoica and R. Moses, *Introduction to Spectral Analysis*. Engle-wood Cliffs, NJ: Prentice-Hall, 2000.
- [14] T. Blu, P. L. Dragotti, M. Vetterli, P. Marziliano, and L. Coulot, "Sparse sampling of signal innovations," *IEEE Signal Processing Magazine*, vol. 25, pp. 31–40, March 2008.